Molecular Biology of the Cell
Vol. 21, 3985–3997, November 15, 2010

# MAL/VIP17, a New Player in the Regulation of NKCC2 in the Kidney

**Monica Carmosino,*† Federica Rizzo,† Giuseppe Procino,† Davide Basco,† Giovanna Valenti,† Biff Forbush,* Nicole Schaeren-Wiemers,‡ Michael J. Caplan,* and Maria Svelto†§**

*Department of Cellular and Molecular Physiology, Yale University School of Medicine, New Haven, CT 06511; †Department of General and Environmental Physiology, University of Bari, 70126 Bari, Italy; §Centro di Eccellenza di Genomica in campo Biomedico ed Agrario (CEGBA), 70126 Bari, Italy; and ‡Department of Biomedicine, University Hospital Basel, 4031 Basel, Switzerland

Submitted May 21, 2010; Revised September 3, 2010; Accepted September 9, 2010
Monitoring Editor: Keith E. Mostov

**The renal-specific $Na^+$-$K^+$-$2Cl^-$ cotransporter (NKCC2) is the major salt transport pathway of the apical membrane of the mammalian thick ascending limb of Henle's loop. Here, we analyze the role of the tetraspan protein myelin and lymphocytes-associated protein (MAL)/VIP17 in the regulation of NKCC2. We demonstrated that 1) NKCC2 and MAL/VIP17 colocalize and coimmunoprecipitate in Lilly Laboratories cell porcine kidney cells (LLC-PK1) as well as in rat kidney medullae, 2) a 150-amino acid stretch of NKCC2 C-terminal tail is involved in the interaction with MAL/VIP17, 3) MAL/VIP17 increases the cell surface retention of NKCC2 by attenuating its internalization, and 4) this coincides with an increase in cotransporter phosphorylation. Interestingly, overexpression of MAL/VIP17 in the kidney of transgenic mice results in cysts formation in distal nephron structures consistent with the hypothesis that MAL/VIP17 plays an important role in apical sorting or in maintaining the stability of the apical membrane. The NKCC2 expressed in these mice was highly glycosylated and phosphorylated, suggesting that MAL/VIP17 also is involved in the stabilization of NKCC2 at the apical membrane in vivo. Thus, the involvement of MAL/VIP17 in the activation and surface expression of NKCC2 could play an important role in the regulated absorption of $Na^+$ and $Cl^-$ in the kidney.**

## INTRODUCTION

The renal-specific $Na^+$-$K^+$-$2Cl^-$ cotransporter (NKCC2) localizes to the apical membranes of TAL cells in the mammalian kidney, where it is responsible for $Na^+$ and $Cl^-$ reabsorption and the maintenance of normal blood pressure. The central role of the NKCC2 in the vectorial transepithelial salt reabsorption along the loop of the Henle is evidenced by the effects of loop diuretics, the pharmacological inhibitors of NKCC2, that are among the most powerful antihypertensive drugs available to date. Genetic mutations of the NKCC2 encoding gene have been shown to impair the function and the apical targeting of NKCC2. The resulting phenotype, known as type I Bartter's syndrome, is characterized by a severe volume depletion, hypokalemia and metabolic alkalosis with high prenatal mortality (Simon *et al*., 1996). Along with mutations resulting in the loss-of-function of the cotransporter, others have been identified that disturb its intracellular trafficking (Pressler *et al*., 2006).

Moreover, progression from prehypertensive to hypertensive state in spontaneously hypertensive rats (SHRs) is accompanied by an increase in steady state protein levels of NKCC2 and its distribution to plasma membrane compared with control rats (Sonalker *et al*., 2004, 2007). Interestingly, the same amount of NKCC2 m-RNA has been found in both strains, suggesting that the NKCC2 over expression was due to a greater translational efficiency or an enhanced stability of the cotransporter in SHRs.

In addition, TAL tubules from Dahl salt-sensitive (DS) rats, a model of salt-dependent hypertension, exhibited significantly higher NKCC2 activity than Dahl salt-resistant strain. Western blot analysis revealed that NKCC2 possessed a different pattern of glycosylation in DS rats, suggesting that NKCC2 might accumulate at different stages of its biosynthesis or degradation in these rats (Alvarez-Guerra and Garay, 2002). These findings underline the need to analyze the molecular mechanisms involved in the intracellular trafficking and membrane stability of NKCC2 to gain insight into the pathophysiology of salt and water retention.

This article was published online ahead of print in *MBoC in Press* (http://www.molbiolcell.org/cgi/doi/10.1091/mbc.E10–05–0456) on September 22, 2010.

Address correspondence to: Monica Carmosino (carmosino@yale.edu).

Abbreviations used: CD, cluster of differentiation; DRM, detergent-resistant membrane; HEK, human embryonic kidney; LLC-PK1, Lilly Laboratories cell porcine kidney; MAL, myelin and lymphocytes-associated protein; MARVEL, mal and related proteins for vesicle trafficking and membrane link; MDCK, Madin-Darby canine kidney; NKCC2, $Na^+$-$K^+$-$2Cl^-$ cotransporter; PP1, protein phosphatase type 1; ROMK, renal outer medullary potassium; SPAK, STE20/SPS1-related proline/alanine-rich kinase; VIP17, vesicular integral protein of 17 kDa.



Supplemental Material can be found at:
http://www.molbiolcell.org/content/suppl/2010/09/21/E10-05-0456.DC1

It is becoming increasingly clear that ion transport proteins do not exist as isolated units in the membranes of living cells. Instead, they seem to participate in an extremely wide array of interactions that help to determine their localization, life span, and susceptibility to control by signals transduction machinery.

A new class of interactions has recently been shown to be relevant to a broad cross-section of renal transport systems. It has been found that several transport proteins, including the aquaporin 2 (AQP2) water channel (Kamsteeg *et al.*, 2007), the $Na^+$,$K^+$-ATPase (Pagel *et al.*, 2003) and the $H^+$,$K^+$-ATPases (Duffield *et al.*, 2003), interact with members of the tetraspan family of membrane proteins. Furthermore, these interactions seem to play important roles in determining the distribution, stability and regulatory properties of these ion transport proteins.

For example, the tetraspan CD63 has been shown to bind directly to the $\beta$-subunit of the $H^+$,$K^+$-ATPase in parietal cells of the rat stomach and to be involved in the regulation of $H^+$,$K^+$-ATPase trafficking. When coexpressed with CD63, the $H^+$,$K^+$-ATPase $\beta$-subunit is rapidly endocytosed and accumulates in intracellular vesicles. In contrast, in the absence of CD63, the $H^+$,$K^+$-ATPase $\beta$-subunit accumulates at the plasmalemma (Duffield *et al.*, 2003).

Moreover, even in the absence of protein-protein interaction, CD63 plays a role in the regulation of renal outer medullary potassium (ROMK) channels. In fact, CD63, interacting with c-Src protein-tyrosine kinase, enhances the inhibitory effect of this kinase on ROMK channels activity (Lin *et al.*, 2008).

The myelin and lymphocyte-associated protein (MAL), also known as vesicle integral protein of 17 kDa (VIP17), in renal epithelial cells is detected exclusively in the apical plasma membranes (Cheong *et al.*, 1999; Puertollano *et al.*, 1999). This protein is heavily expressed in distal nephron segments, TAL, and distal convoluted tubules, as well as in collecting tubules (Frank *et al.*, 1998). MAL/VIP17 joins a growing group of tetraspan membrane proteins and is related to the MARVEL domain-containing class of polypeptide (*ma*l and *r*elated proteins for *ve*sicle trafficking and membrane *l*ink) (Sánchez-Pulido *et al.*, 2002).

Interestingly, overexpression of MAL/VIP17 in the kidney of transgenic mice results in dramatic amplification of the apical surface and ultimately to cysts formation in distal nephron structures, consistent with the hypothesis that it plays an important role in apical sorting or in maintaining the stability of the apical membranes (Frank *et al.*, 2000).

MAL/VIP17 seems to be associated with and required for the formation of the detergent insoluble structures variously referred to as "rafts" or glycolipid- and cholesterol-enriched membranes. Moreover, recent reports demonstrated that MAL/VIP17 clusters, formed either by spontaneous clustering of MAL/VIP17 or by antibody-mediated cross-linking of FLAG-tagged MAL/VIP17, laterally concentrate markers of sphingolipid rafts in COS cells, placing MAL/VIP17 as a key component in the organization of membrane rafts domains (Goldstein Magal *et al.*, 2009). MAL/VIP17 interacts with glycosylphosphatidylinositol (*GPI*)-anchored proteins and may either escort its associated proteins to the apical membrane or it may retain associated proteins within the apical membrane (Cheong *et al.*, 1999; Puertollano *et al.*, 1999; Kamsteeg *et al.*, 2007; Ramnarayanan *et al.*, 2007).

In this study, we analyzed the interaction of MAL/VIP17 and NKCC2 and the possible physiological role of MAL/VIP17 in the trafficking and function of NKCC2. Because NKCC2 is difficult to express in epithelial cells, little is known about mechanisms that govern the intracellular trafficking and membrane stability of this cotransporter. Indeed, we previously generated a chimeric NKCC2 protein that accumulates at the apical membranes of stably transfected renal epithelial cells that allows us to explore factors that regulate NKCC2 sorting and function (Carmosino *et al.*, 2008).

Using LLC-PK1 cells coexpressing a chimeric NKCC2 construct and MAL/VIP17, we showed that MAL/VIP17 stabilized NKCC2 at the apical membrane. Experiments performed in both MAL/VIP17-MDCK deplete cells and MAL/VIP17-overexpressing mice corroborated this hypothesis.

## MATERIALS AND METHODS

### *Constructs and Antibodies*

FLAG-MAL/VIP17 construct has been generated as described previously (Kamsteeg *et al.*, 2007). The chimeric NKCC2 construct used in this work is named c-NKCC2 and corresponding to the chimera IV-V described previously (Carmosino *et al.*, 2008).

The monoclonal T4 antibody was from Developmental Studies Hybridoma Bank (University of Iowa, Iowa City, IA). The polyclonal R5 antibody was generated and characterized by Prof. Biff Forbush (Yale University, New Haven, CT). The polyclonal anti-MAL/VIP17 antibody was from Abcam (Cambridge, MA). The rabbit polyclonal anti-flotillin-2 and the goat polyclonal anti-actin antibodies were from Santa Cruz Biotechnology (Santa Cruz, CA). The monoclonal anti-hemagglutinin (HA) antibody and both the monoclonal and polyclonal anti-FLAG antibodies were from Sigma-Aldrich (St. Louis, MO).

### *Cell Culture, Transfection, and Animals*

LLC-PK1 cells were maintained in DMEM, 2 mM L-glutamine, 10% fetal bovine serum, penicillin (50 U/ml), and streptomycin (50 U/ml) at 37°C, 5% $CO_2$ in a humidified incubator. For transfection, cells were grown until ~95% confluent and then cotransfected with HA-tagged c-NKCC2 and with FLAG-tagged MAL/VIP17. Lipofectamine 2000 (Invitrogen, Carlsbad, CA) was used for transfection according to the manufacturer's instructions. Stable clones were selected in 1 mg/ml geneticin (for cells transfected with HA-tagged c-NKCC2) and 0.2 mg/ml hygromycin B (for cells transfected with FLAG-tagged MAL/VIP17).

Kidneys of Wistar-Kyoto rats (from Harlan, Indianapolis, IN) and of transgenic MAL/VIP17-overexpressing mice (from Dr. Nicole N. Schaeren-Wiemers, University Hospital Basel, Basel, Switzerland) were used in this work.

### *MAL/VIP17 Silencing in Madin-Darby Canine Kidney (MDCK) Cells*

A stealth small interfering RNA (siRNA) from Invitrogen targeting dog MAL/VIP17 was used in combination with Lipofectamine 2000 reagent to knock down MAL/VIP17 expression in MDCK cells. The relative amounts of siRNA and Lipofectamine 2000 used in each experiment were decided according to the number of plated cells and to the guidelines provided from Invitrogen. When confluent at 70%, MDCK were treated twice on two consecutive days with either scrambled MAL/VIP17 siRNA (MOCK) or MAL/VIP17 siRNA (MAL/VIP KD).

To analyze MAL/VIP17 knock down, a 60-mm plate of either KD or mock MDCK cells was lysed in lysis buffer containing 1% Triton X-100 at 4°C. The lysates was passed through a 22-gauge needle several times. The detergent-insoluble material was then collected after centrifugation at 13,000 rmp for 15 min. This material was further incubated in lysis buffer supplemented with 60 mM octylglucoside at 37°C for 30 min. After centrifugation at 13,000 rmp for 15 min, the supernatant was recovered and used for the analysis of MAL/VIP17 expression by SDS-polyacrylamide gel electrophoresis (PAGE) and Western blotting.

Western blotting was performed using the 2E5 antibody, a rat anti-dog MAL/VIP17 antibody, kindly provided by Prof. Miguel Alonso (University of Madrid, Madrid, Spain) and characterized previously in MDCK cells (Puertollano *et al.*, 1999).

### *Immunofluorescence*

Kidneys from rats and mice were fixed in paraformaldehyde 4% in phosphate-buffered saline (PBS) and than cryoprotected by incubation overnight in sucrose 30% in PBS. Sections of 5 $\mu$m were cut and mounted on Superfrost Plus glass. After three washes in PBS, sections were blocked in saturation buffer (1% bovine serum albumin in PBS) for 20 min at room temperature (RT) and incubated with the primary antibodies for 2 h at RT (R5, 1:1000; MAL/VIP17, 1:500) in saturation buffer. After three washes in PBS, sections were incubated with the appropriate Alexa Fluor-conjugated secondary antibodies for 1 h at RT.

LLC-PK1–transfected cells, grown on 0.4-$\mu$m cell culture inserts, were fixed in methanol for 5 min and then subjected to immunofluorescence as described above. Primary antibodies used were as follows: monoclonal anti-HA antibody 1:1000 to detect c-NKCC2 and the polyclonal anti-FLAG antibody 1:1000

to detect MAL/VIP17. Confocal images were obtained with a laser scanning fluorescence microscope (TSC-SP2; Leica Microsystems, Deerfield, IL).

### *Tissues Homogenization and Fractionation*

Whole rat kidney was homogenized in ice-cold anti-phosphatase buffer (150 mM NaCl, 30 mM NaF, 5 mM EDTA, 15 mM $Na_2HPO_4$, 15 mM pyrophosphate, and 20 mM HEPES, pH 7.2) with 2% 3-[(3-cholamidopropyl)dimethylammonio]propanesulfonate (CHAPS) by using 25 strokes at 25,000 rpm with a Polytron tissue homogenizer (Brinkmann Instruments, Westbury, NY) and centrifuged for 10 min at 4000 × *g* at 4°C to pellet debris. Supernatant was centrifuged for 40 min at 20,000 × *g* at 4°C, and the resulting membranes containing pellet were resuspended in anti-phosphatase buffer. Membranes were then used for coimmunoprecipitation (coIP) experiments.

Kidneys of control and MAL/VIP17-overexpressing mice were homogenized in ice-cold anti-phosphatase buffer with 1% Triton X-100 and 0.5 μM calyculin A (CalA) by using Dounce homogenizer. After 30 min of lysis on ice, lysates were clarified by centrifugation at 13,000 × *g* for 30 min at 4°C. Lysates were resolved on NuPAGE gels (Invitrogen) and after transfer to Immobilon P membrane, lanes they were probed with antibodies against: phosphorylated NKCC2 (R5, 1:1000), total NKCC2 (T4, 1:1000), actin (1:500), and MAL/VIP17 (1:500).

### *Coimmunoprecipitation Experiments*

Rat kidney membranes were precleared with 100 μl of protein A-Sepharose suspension (Sigma-Aldrich) for 1 h at 4°C and then incubated with rabbit polyclonal antibody to MAL/VIP17 overnight at 4°C under rotation. Immunocomplexes were bound using 100 μl of protein A-Sepharose suspension for 2 h at 4°C under rotation and than washed five times with anti-phosphatase buffer. Immunocomplexes were dissociated in NuPage LDS sample buffer (Invitrogen) with 100 mM dithiothreitol (DTT), heated at 95°C for 10 min, and resolved on gel. After transfer to Immobilon P membrane, lanes were probed with antibodies against NKCC2 (T4, 1:1000) and MAL/VIP17 (MAL/VIP17 rabbit polyclonal antibody, 1:1000).

LLC-PK1 cells cotransfected with c-NKCC2 and MAL/VIP17 were washed in ice-cold PBS-CM and scraped in anti-phosphatase buffer with 2% CHAPS. Lysates were clarified by centrifugation at 13,000 × *g* for 15 min at 4°C, supernatants were precleared with protein A-Sepharose suspension and then incubated with the polyclonal anti-FLAG antibody (1:1000) overnight at 4°C under rotation to immunoprecipitate MAL/VIP17. Immunocomplexes were bound using protein A-Sepharose suspension, washed, dissociated in NuPage LDS sample buffer, and resolved on NuPAGE gels. After transfer the membrane was incubated with antibodies against NKCC2 (T4, 1:1000) and MAL/VIP17 (monoclonal anti-FLAG, 1:1000).

### *Floatation Assay on Discontinuous OptiPrep Gradient and Detergent Solubility Assay*

Transfected LLC-PK1 cells grown on 10-cm-diameter Petri dishes were washed and scraped in PBS and centrifuged at 1500 × *g* for 5 min. The pellet was resuspended in isolation medium (150 mM NaCl, 5 mM EDTA, and 25 mM Tris-HCl, pH 7.4, supplemented with protease inhibitors) containing 2% CHAPS and incubated for 30 min on ice. Two volumes of OptiPrep was added to 1 volume of lysate and laid at the bottom of an ultracentrifuge tube. Then, 2 volumes of 35, 30, 25, and 20% (wt/vol) OptiPrep in isolation medium was gently overlaid on top of the sample and gradient centrifuged at 160,000 × *g* for 4 h at 4°C. Twenty-two fractions of equal volume were collected from top to bottom of the tube. Ten microliters of each fraction was separated on NuPAGE gels and assessed by Western blotting for the presence of NKCC2 (T4, 1:1000), MAL/VIP17 (monoclonal anti-FLAG antibody, 1:1000), and flotillin-2 (anti flotillin-2 antibody, 1:500).

Alternatively, cell lysates were centrifuged at 4°C for 1 h at 100,000 × *g*. The soluble (supernatant) and insoluble (pellet) fractions (10 μg of total proteins) were separated on NuPAGE gels and assessed by Western blotting for the presence of the proteins described above.

### *Endocytosis Assay*

Endocytosis assays were performed as described previously (Procino *et al.*, 2010). In brief, cells grown to confluence were biotinylated with cell-impermeable NHS-SS-biotin from the apical side. Cells were returned to 37°C, to permit internalization of surface proteins, for 1 or 2 h. Next, cells were washed with ice-cold PBS-CM and treated 3 × 20 min with ice-cold 150 mM MesNa in 100 mM NaCl, 1 mM EDTA, 50 mM Tris (pH 8.6), 0.2% BSA. The cell-impermeable MesNa removes cell surface-bound biotin, whereas internalized biotinylated proteins are protected. Excess of MesNa was quenched with ice-cold 120 mM iodoacetic acid in PBS-CM, and cells were lysed. Lysates were sonicated for 30 s, incubated at 37°C for 20 min and unsolubilized material was pelleted at 13000 *g* for 10 min. Biotinylated proteins were precipitated with streptavidin beads suspension under rotation at 4°C overnight. Beads were washed and biotinylated proteins were extracted in NuPAGE LDS sample buffer with 100 mM DTT, heated at 95°C for 10 min and resolved on NuPAGE gels. After transfer Immobilon P membrane was probed with antibody T4 against NKCC2 (1:1000).

### *Activation Assay*

Cells were preincubated for 30 min in basic medium (135 mM NaCl, 1 mM $MgCl_2$, 1 mM $Na_2SO_4$, 1 mM $CaCl_2$, and 15 mM Na-HEPES, pH 7,4). Then, they were incubated for 30 min in low $Cl^-$ medium (1 mM NaCl, 1 mM $MgCl_2$, 1 mM $Na_2SO_4$, 1 mM $CaCl_2$, 15 mM Na-HEPES, and 134 mM Na-gluconate, pH 7,4) or for 15 min in basic medium with 0.5 μM protein phosphatase-1 inhibitor calyculin A (Sigma-Aldrich). After the incubation, cells were scraped in anti-phosphatase buffer. After lysis on ice for 30 min, lysates were sonicated and unsolubilized material was pelleted at 13,000 × *g* for 15 min. Proteins were extracted in NuPAGE LDS sample buffer with 50 mM DTT, heated at 70°C for 10 min, and resolved on NuPAGE gels. After transfer on membrane lanes were probed with antibody against phosphorylated NKCC2 (R5, 1:1000) and total NKCC2 (T4, 1:1000).

### *Deglycosylation Assay*

Proteins (100 μg) from lysates of MAL/VIP17-overexpressing mice kidneys were denaturated in a final volume of 15 μl of SDS 1% in PBS for 10 min at 99°C. After denaturation, 15 μl of PBS supplemented with protease inhibitors and 1 μl of PNGase F (Sigma-Aldrich), were added, and samples were incubated for 3 h at 37°C. Proteins were extracted in NuPAGE LDS sample buffer with 50 mM DTT, heated at 70°C for 10 min, and resolved on NuPAGE gels. After transfer membrane was probed with antibody T4 against NKCC2 (1:1000).

## RESULTS

### *MAL/VIP17 and NKCC2 Colocalize and Coimmunoprecipitate in Renal TAL Cells*

Previous studies demonstrated that MAL/VIP17 colocalizes in kidneys with Calbindin-28k, a marker for the connecting tubule, and AQP2, a marker of principal collecting duct cells (Kamsteeg *et al.*, 2007). We performed colocalization experiments in rat kidney sections to verify whether NKCC2 and MAL/VIP17 colocalize in the TAL. To label NKCC2, we used the polyclonal R5 antibody, which was specifically raised against a sequence in the NKCC2 N terminus that contains regulatory phospho-threonines. The utility of this antibody for immunofluorescence analysis has been well established (Gimenez and Forbush, 2003). An anti MAL/VIP17 polyclonal antibody was used to detect MAL/VIP17. Because both antibodies used were generated in rabbits, comparison of tubular localization of NKCC2 and MAL/VIP17 was undertaken using adjacent, serial kidney sections. NKCC2 (green) and MAL/VIP17 (red) seemed to be expressed in the same tubular structures. The separate images were merged, showing that NKCC2 and MAL/VIP17 colocalized at the apical membranes of TAL cells (Figure 1A).

To analyze whether MAL/VIP17 and NKCC2 interact in vivo, we solubilized membranes of kidney medullae by using 2% CHAPS and used them as starting material for coIP. Immunoprecipitation with MAL/VIP17 antibodies and subsequent immunoblotting for NKCC2 using the monoclonal T4 antibody revealed that NKCC2 indeed coimmunoprecipitated with MAL/VIP17. A nonimmune serum (a polyclonal anti-AQP4 antibody) was used a negative control (n.s.). The Western blotting profile of NKCC2 in kidney rat membranes clearly showed different bands corresponding to NKCC2 in different stages of maturation. Coimmunoprecipitation experiments showed that MAL/VIP17 preferentially interacted with the most highly glycosylated form of NKCC2 (Figure 1A′, NKCC2, MAL/VIP17). After being probed with T4 antibody, membranes were stripped and incubated with R5 antibody to verify whether NKCC2 also coimmunoprecipitated with the phosphorylated form of NKCC2. As shown in Figure 1A′, the most highly glycosylated form of NKCC2 is also phosphorylated and coimmunoprecipitated with MAL/VIP17 (Figure 1A′, p-NKCC2). We conclude, therefore, that NKCC2 and MAL/VIP17 colocalize and interact at the apical membranes of renal TAL cells.

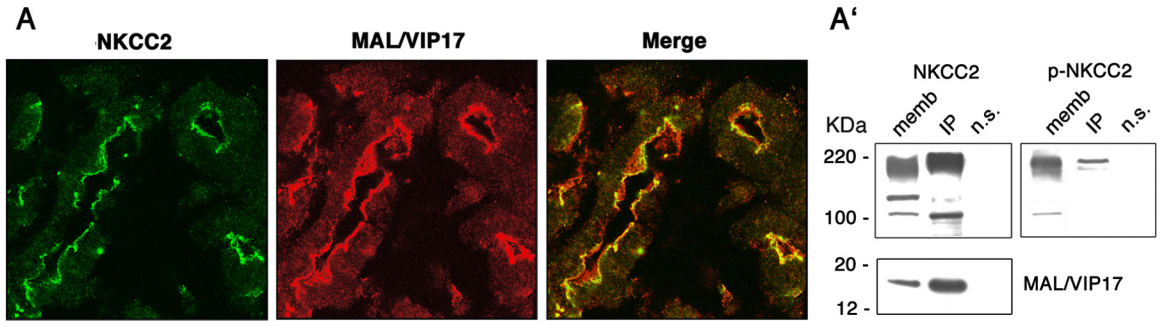


**Figure 1.** Colocalization and coimmunoprecipitation experiments in rat kidney medulla. (A) Sequential sections of rat kidney were stained for NKCC2 (green) and MAL/VIP17 (red). The image merge showed that NKCC2 codistributes with MAL/VIP17. (A′) Rat kidney medullae membranes were solubilized in CHAPS and subjected to immunoprecipitation using MAL/VIP17 antibody. Western blotting on kidney membranes (memb) and Immunoprecipitates (IP) showed that NKCC2 coimmunoprecipitated with MAL/VIP17 (NKCC2). A nonimmune serum (a polyclonal anti-AQP4 antibody) was used as negative control (n.s.). The same membrane was stripped and subjected to Western blotting with R5 antibody, showing that also the phosphorylated form of NKCC2 coimmunoprecipitated with MAL/VIP17 (p-NKCC2).

### *MAL/VIP17 Interacts with c-NKCC2 in Renal Transfected Epithelial Cells and Is Not Involved in the Targeting of NKCC2 to the Apical Surface*

To analyze the role of MAL/VIP17 in the intracellular trafficking of NKCC2, we stably transfected LLC-PK1 cells with an engineered NKCC2 construct. LLC-PK1 cells are derived from porcine renal proximal tubule cells that do not express MAL/VIP17 (Frank *et al.*, 1998). Accordingly, MAL/VIP17 was undetectable in LLC-PK1 cells when assayed by Northern blotting (Kamsteeg *et al.*, 2007). For these reasons, we believed that this cell line was a suitable cellular model to analyze the effect of the ectopic expression of MAL/VIP17 on the trafficking of NKCC2.

It is well known that NKCC2 is difficult to express stably in epithelial cells. We previously generated a construct in which the apical sorting determinants of NKCC2 were exchanged into the corresponding region of the NKCC1 C-terminal tail. The resulting chimera (c-NKCC2) was functionally active and accumulated at the apical membranes of stably transfected renal epithelial cells (Carmosino *et al.*, 2008).

Therefore, to achieve the goal of this study we generated a c-NKCC2 stably transfected LLC-PK1 cell line in which exogenous MAL/VIP17 was coexpressed when required. c-NKCC2 and MAL/VIP17 are both tagged at their extreme N-terminal tails with HA tag and FLAG tag, respectively. Epitopes were shown previously to not disturb the sorting and function of both proteins (Puertollano *et al.*, 1999; Carmosino *et al.*, 2008). Immunofluorescence experiments showed that c-NKCC2 and MAL/VIP17 colocalized at the apical membrane of LLC-PK1 cells. Moreover, they showed that c-NKCC2 accumulated at the apical membranes of LLC-PK1 cells regardless of whether exogenous MAL/VIP17 was coexpressed, suggesting that MAL/VIP17 is not required for the apical sorting of NKCC2 (Figure 2A).

Coimmunoprecipitation experiments were carried out to verify whether MAL/VIP17 and c-NKCC2 interact in LLC-PK1 cells. A polyclonal anti-FLAG antibody was used to immunoprecipitate MAL/VIP17, and the monoclonal T4 antibody to check for the presence of c-NKCC2 by Western blotting.

The T4 monoclonal antibody in LLC-PK1 cells, as well as in many other cell types (Flemmer *et al.*, 2002; Liedtke *et al.*, 2005; Carmosino *et al.*, 2008), identifies two bands ranging from 160 to 130 kDa corresponding to a fully and poorly glycosylated NKCC, respectively. As shown in Figure 2A′, MAL/VIP17 coimmunoprecipitated with the fully glycosylated form of c-NKCC2 when coexpressed in LLC-PK1 cells (Figure 2A′, IP), indicating that MAL/VIP17 and c-NKCC2 interact at the apical membrane.

To further verify whether MAL/VIP17 is involved in the apical sorting of NKCC2, we knocked down MAL/VIP17 expression in c-NKCC2–transfected MDCK cells, which endogenously expressed MAL/VIP17. The apical localization of c-NKCC2 was not affected by MAL/VIP17 depletion confirming the data obtained in LLC-PK1 cells (Figure 2B). Western blotting of MAL/VIP17 in detergent-resistant membrane (DRM) fractions prepared from MDCK, confirmed a significant decrease in the MAL/VIP17 expression in knocked down cells (Figure 2B′, MDCK DRMs, MAL/VIP17), by ~70% as quantified by the densitometric analysis of MAL/VIP17 band (Figure 2B′, MAL/VIP17 densitometry). Flotillin-2 was used as marker of DRMs and as protein loading control (Figure 2B′, MDCK DRMs, Flo-2).

### *The C-Terminal Region of NKCC2, Containing the Apical Sorting Determinants, Is Involved in the Interaction with MAL/VIP17*

To verify whether the interaction between MAL/VIP17 and NKCC2 was specific, we cotransfected MAL/VIP17 with the secretory isoform NKCC1 in LLC-PK1 cells. As expected, NKCC1 was expressed along the basolateral membrane in LLC-PK1 cells (Figure 2C). Coimmunoprecipitation experiments demonstrated that MAL/VIP17 did not interact with NKCC1 (Figure 2C′), indicating that the interaction between c-NKCC2 and MAL/VIP17 is specific. An alternative explanation for this result is that, although MAL/VIP17 and NKCC1 could be able to interact, they are expressed in distinct membrane domains in polarized epithelial cells (apical for MAL/VIP17 and basolateral for NKCC1). To test this possibility, we cotransfected MAL/VIP17 and NKCC1 in unpolarized human embryonic kidney (HEK)-293 cells. Interestingly, they did not coimmunoprecipitate even when expressed in these cells in which they did colocalize at the plasma membrane (Supplemental Figure 1). These results clearly showed that the interaction between MAL/VIP17 and c-NKCC2 is actually specific. Because c-NKCC2 is a chimeric protein between NKCC1 and NKCC2, we can conclude that the 150-amino acid stretch of the NKCC2 C-terminal tail present in the chimera is indeed the region of NKCC2 necessary for the interaction with MAL/VIP17 (Figure 2A′, chimera structure).

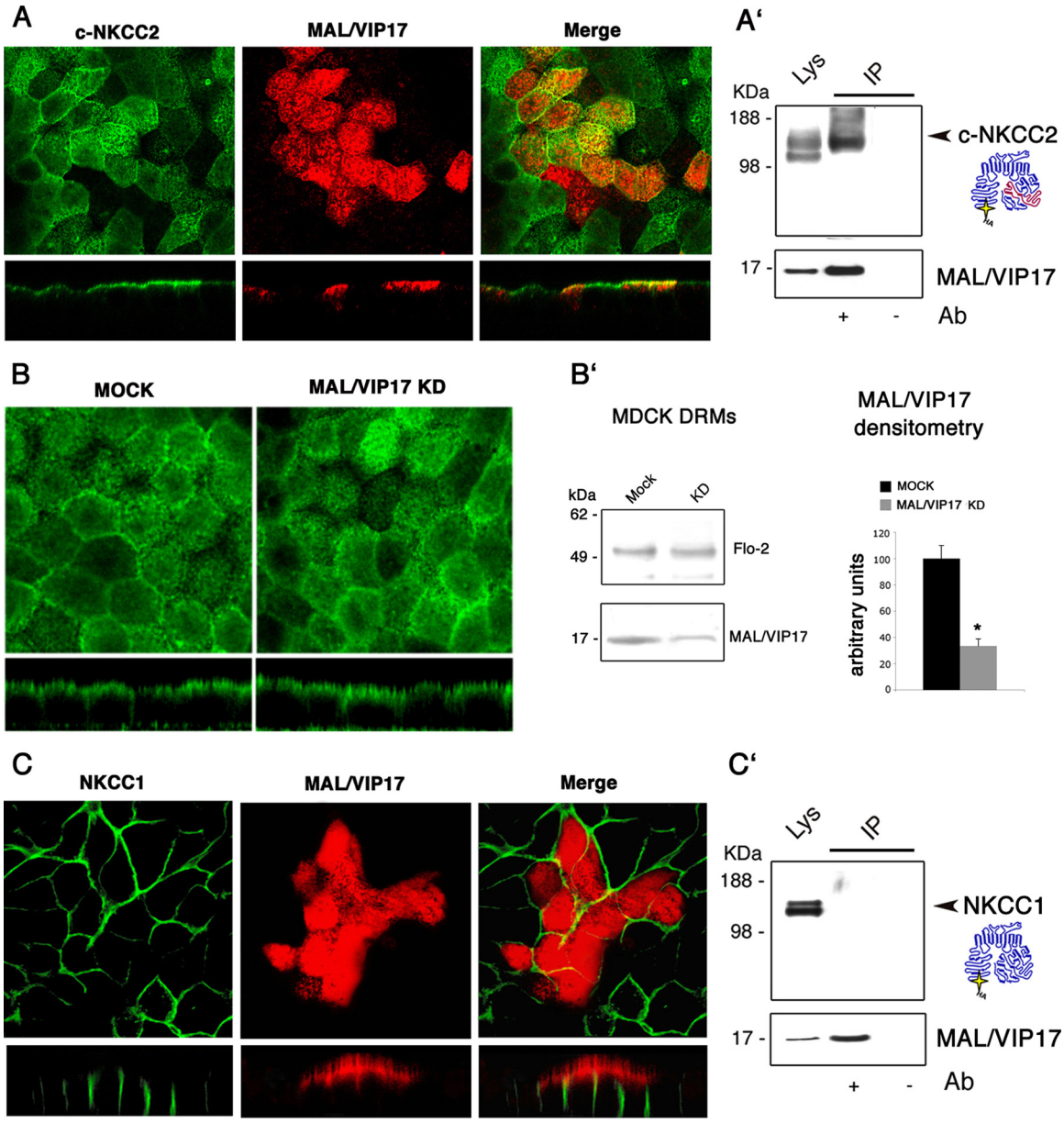


**Figure 2.** c-NKCC2 expression in LLC-PK1 and MDCK cells. (A) LLC-PK1 cells stably expressing c-NKCC2 were transfected with MAL/VIP17. Colocalization experiments were then performed using a monoclonal anti-HA antibody to stain c-NKCC2 (green) and a polyclonal anti-FLAG antibody to stain MAL/VIP17 (red). The merge showed that c-NKCC2 and MAL/VIP17 colocalize at the apical membrane. (A′) The same cells were lysed in CHAPS and subjected to immunoprecipitation with the polyclonal anti-FLAG antibody. Western blotting analysis using T4 antibody showed that c-NKCC2 coimmunoprecipitated with MAL/VIP17. The structure of the c-NKCC2 construct is shown on the right of the corresponding Western blotting. The NKCC1 regions are shown in blue, and the NKCC2 regions are shown in red. (B) Endogenously expressed MAL/VIP17 was knocked down by siRNA in c-NKCC2-transfected MDCK cells. Immunofluorescence showed that c-NKCC2 was expressed at the apical membrane in both control (MOCK) and MAL/VIP17 knocked down cells (MAL/VIP17 KD). (B′) Western blotting of MAL/VIP17 and flotillin-2 (Flo-2) in DRM fractions prepared from MDCK (MDCK DRMs). The densitometric analysis of the MAL/VIP17 bands showed a decrease of ~70% of MAL/VIP17 expression in MAL/VIP7 knocked down cells (MAL/VIP17 densitometry). Student's *t* test, *$p < 0.0001$. (C) LLC-PK1 cells stably expressing NKCC1 were transfected with MAL/VIP17. The merge showed that NKCC1 and MAL/VIP17 did not colocalize. (C′) The same cells were lysed in CHAPS and subjected to immunoprecipitation with the polyclonal anti-FLAG antibody. Western blotting analysis using T4 antibody showed that NKCC1 did not coimmunoprecipitate with MAL/VIP17.

### *MAL/VIP17 Decreases the Internalization of c-NKCC2*

It has been demonstrated that the MAL/VIP17's primary role in the apical sorting of AQP2 may be attributable to the stabilization and retention of AQP2 at the apical surface rather then to any involvement in its apical delivery (Kamsteeg *et al.*, 2007). To verify whether this is also true for NKCC2, we performed an internalization assay for c-NKCC2 on LLC-PK1 cells in the presence (+ MAL/VIP17) and in the absence (− MAL/VIP17) of MAL/VIP17. Cells were biotinylated at 4°C on their apical surfaces with cleavable biotin, returned to 37°C to allow internalization, and then treated with the membrane-impermeant reducing agent MesNa. Internalized

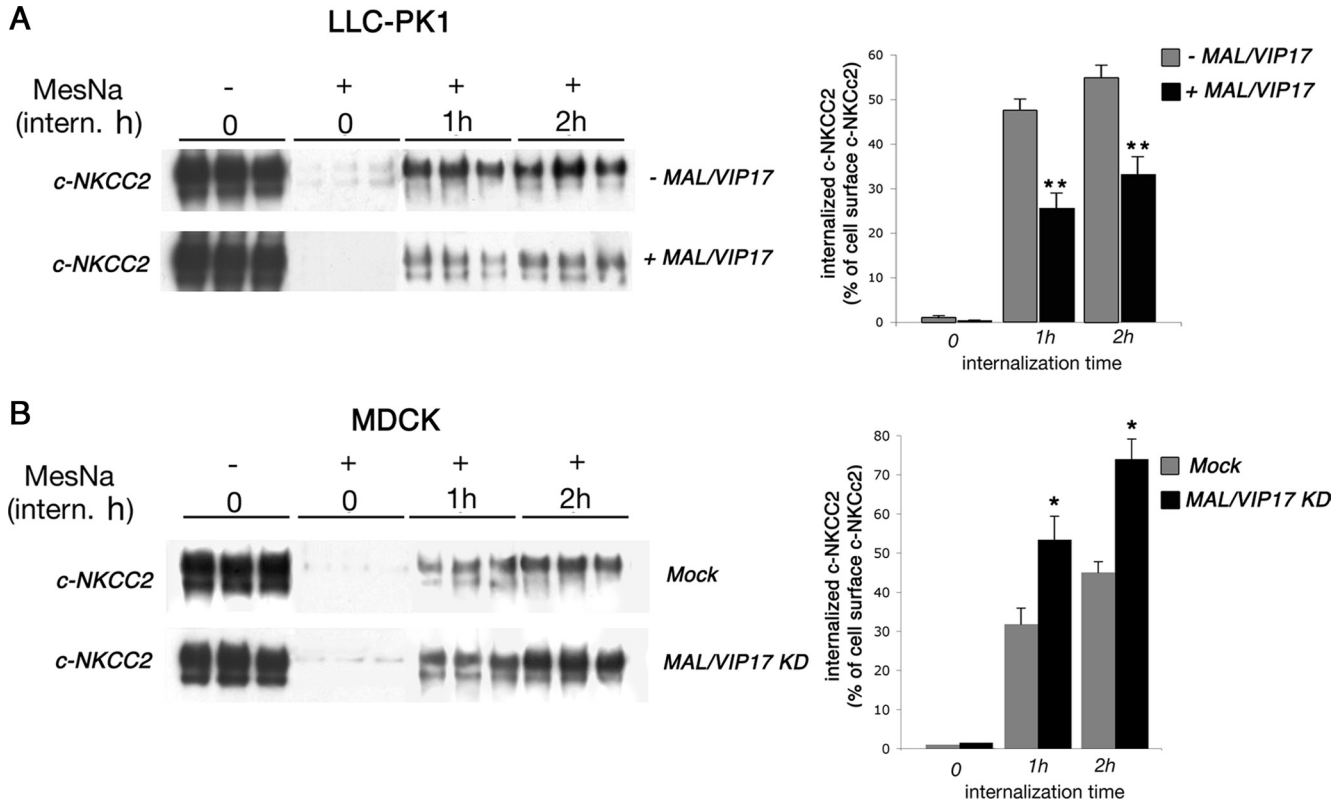


**Figure 3.** Internalization experiments. (A) LLC-PK1 cells expressing c-NKCC2 alone or in combination with MAL/VIP17 were grown to confluence and biotinylated from their apical side by using a cleavable biotin. Cells were then allowed to internalize surface-labeled proteins for the indicated times. The remaining surface accessible biotin was then stripped with MesNa where indicated (MesNa, +). Biotinylated proteins were then recovered and immunoblotted for NKCC2. Each experimental condition was examined in triplicate. Internalized c-NKCC2 was determined from three independent experiments by densitometry of biotinylated c-NKCC2 at 1 and 2 h of internalization and expressed as percentage of total cell surface c-NKCC2 (MesNa −, intern. h 0). Student's *t* test, $^{**}p < 0.0001$. (B) Control (mock) and MAL/VIP17 knocked down (MAL/VIP17 KD) MDCK cells were subjected to the same assay described above. Each experimental condition was examined in triplicate. Internalized c-NKCC2 was determined from three independent experiments by densitometry of biotinylated c-NKCC2 at 1 and 2 h of internalization and expressed as percentage of total cell surface c-NKCC2 (MesNa −, intern. h 0). Student's *t* test, $^{*}p < 0.005$.

c-NKCC2 was protected from cleavage and thus recovered by immobilized streptavidin. As shown in Figure 3A, more c-NKCC2 was protected from MesNa cleavage at each successive time point (1–2 h) in MAL/VIP17 lacking cells compared with MAL/VIP17-transfected cells. These data suggest that MAL/VIP17 decreases the internalization of c-NKCC2 in LLC-PK1 cells. Interestingly, the knockdown of MAL/VIP17 in MDCK cells increased the rate of c-NKCC2 internalization by ~35% at each successive time points, confirming that MAL/VIP17 is involved in stabilizing NKCC2 at the apical membrane in MDCK as well as in LLC-PK1 cells (Figure 3B).

### *MAL/VIP17-dependent Phosphorylation Dynamics of c-NKCC2: MAL/VIP17 Increases the Fraction of Phosphorylated/Phosphorylatable c-NKCC2*

Three phospho-acceptor threonines in the N terminus of NKCC1 and NKCC2 have been identified as key elements in the NKCC1 cotransporter activation (Darman and Forbush, 2002). Because this region is well conserved both across species and between isoforms, it is an excellent candidate as a universal regulatory motif for NKCCs.

NKCCs are activated under conditions in which cells are depleted of cytosolic chloride, and we have routinely used low $Cl^-$ preincubation to stimulate the chloride transport mediated by NKCCs in mammalian cells (see *Materials and Methods*). To analyze the activation dynamics of c-NKCC2 expressed in LLC-PK1 cells, cells were preincubated for 30 min in basic medium (see *Materials and Methods*). A group of cells were then incubated in low $Cl^-$ medium or with 0.5 $\mu$M CalA, a specific protein phosphatase-1 inhibitor, in basic medium for 30 min. Cells were then lysed and the phosphorylation state of c-NKCC2 was evaluated by Western blotting using the R5 antibody, specifically raised against the conserved phospho-threonines in the N-terminus of NKCCs.

Figure 4A showed that the phosphorylation state of c-NKCC2 increased in LLC-PK1 cell upon ectopic expression of MAL/VIP17 in all the experimental conditions (Figure 4A, CTR, low $Cl^-$, CalA). The amount of total c-NKCC2, revealed using the T4 antibody, was unchanged in all the experimental conditions. Densitometric analysis of the R5 bands, normalized for the T4 signals, showed that the phosphorylation state of c-NKCC2 was significantly increased by 30 ± 0.24, 51.6 ± 0.4, and 42.1 ± 0.3% in control, low chloride, and CalA conditions, respectively, after the ectopic expression of MAL/VIP17 (Figure 4B). In contrast, the knockdown of MAL/VIP17 expression in MDCK cells clearly decreased the phosphorylation state of c-NKCC2 in both control and low $Cl^-$ conditions (Figure 4C). Densitometric analysis of the phosphorylated/phosphorylatable

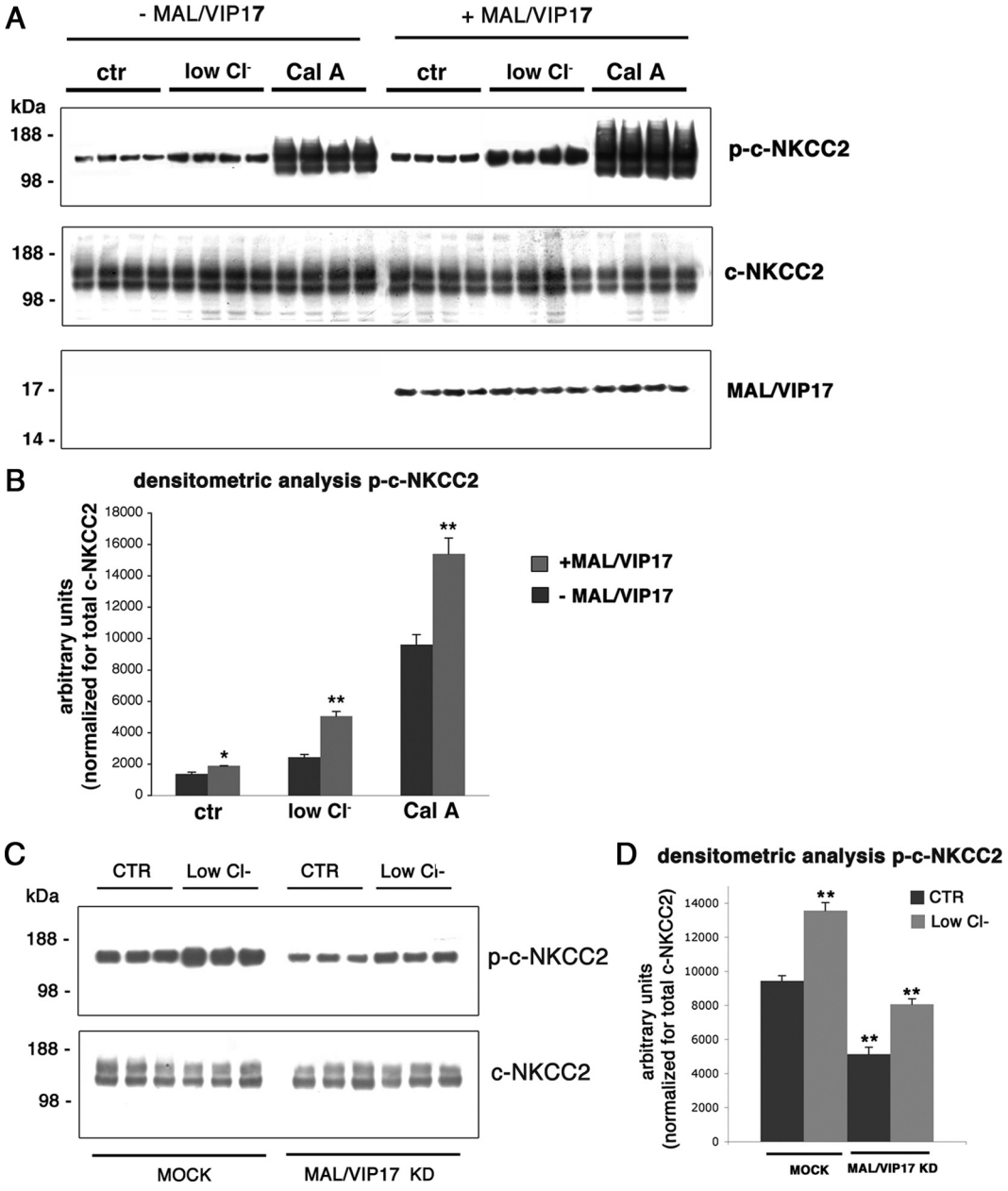


**Figure 4.** Phosphorylation dynamics of NKCC2 in the absence or in the presence of MAL/VIP17. (A) LLC-PK1cells expressing c-NKCC2 alone or in combination with MAL/VIP17 were grown to confluence on 12-well plates, incubated in low $Cl^-$ medium or in the presence of 0.5 $\mu$M CalA. Cells were then lysed and subjected to Western blotting using R5 antibody. The same nitrocellulose membranes were stripped and reprobed by Western blotting with T4 antibody. Each experimental condition was examined in quadruplicate. (B) The quantitation of phosphorylated c-NKCC2 was determined from three independent experiments by densitometry of phospho-c-NKCC2 bands (R5 signal) normalized for the corresponding c-NKCC2 bands (T4 signal). Student's *t* test, *$p < 0.001$, **$p < 0.0001$. (C) Both control (MOCK) and MAL/VIP17-depleted MDCK cells (MAL/VIP17 KD) were incubated in regular or low $Cl^-$ medium. Cells were then lysed and subjected to Western blotting using R5 antibody (p-c-NKCC2). The same nitrocellulose membranes were stripped and reprobed by Western blotting with T4 antibody (c-NKCC2). Each experimental condition was examined in triplicate. (D) The quantitation of phosphorylated c-NKCC2 was determined from three independent experiments by densitometry of phospho-c-NKCC2 bands (p-c-NKCC2) normalized for the corresponding c-NKCC2 bands (c-NKCC2). Student's *t* test, **$p < 0.0001$.

(p)-c-NKCC2 bands, normalized for the total c-NKCC2, showed that in MAL/VIP17-depleted MDCK cells the extent of c-NKCC2 phosphorylation decreased by 44.4 ± 0.3 and 42 ± 0.25% in control and low $Cl^-$ conditions respectively (Figure 4D). Altogether, these results indicate that the presence of MAL/VIP17 increases the fraction of phosphorylated/phosphorylatable c-NKCC2 in both LLC-PK1 and MDCK cells.

One explanation for these results is based on the possibility that MAL/VIP17 preferentially interacts with and stabilizes the phosphorylated form of c-NKCC2. To verify this hypothesis, we performed coimmunoprecpitation experiments either in control or in low $Cl^-$ activated LLC-PK1 cells. As show in Figure 5A, the phosphorylation state of the cotrasporter, analyzed using R5 antibody, increased in low $Cl^-$ condition (lysates, low $Cl^-$) and MAL/VIP17 was able

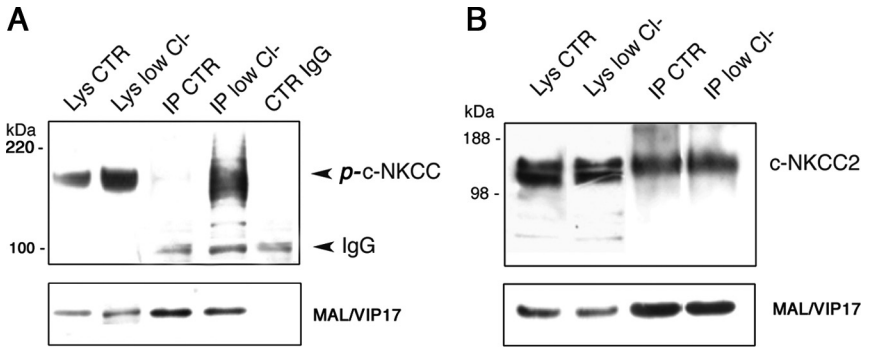


**Figure 5.** Coimmunoprecipitation of c-NKCC2 and MAL/VIP17 in CTR and low $Cl^-$ conditions. LLC-PK1 cells expressing c-NKCC2 and MAL/VIP17 were incubated in CTR or low $Cl^-$ conditions, lysed in 2% CHAPS, and subjected to immunoprecipitatation with anti-FLAG antibody. Western blotting analysis was made with R5 (A) or T4 (B) antibodies. The phosphorylation of the cotransporter in low $Cl^-$ did not change the apparent affinity of c-NKCC2 for MAL/VIP17.

to interact with the phosphorylated form of c-NKCC2 (Figure 5A, IP, low Cl). However, the amount of total c-NKCC2 (detected with T4 antibody) that coimmunoprecipitates with MAL/VIP17 did not increase when cells were incubated in low $Cl^-$ solution (Figure 5B). This suggests that MAL/VIP17 does not preferentially interact with the phosphorylated form of c-NKCC2.

Another possible explanation for the increased phosphorylation of c-NKCC2 in MAL/VIP17-expressing LLC-PK1 cells is that MAL/VIP17 binds both to NKCC2 and to elements of the NKCC2 activation machinery. However, we found that neither the STE20/SPS1-related proline/alanine-rich kinase (SPAK) kinase nor the protein phosphatase-1, the major players in the NKCC activation, coimmunoprecipitate with MAL/VIP17 (Supplemental Figure 2).

### *MAL/VIP17 Is Not Involved in the Association of c-NKCC2 with DRMs*

MAL/VIP17 protein is present in DRMs and interacts with GPI-apical proteins. Indeed, is thought to play a role in the incorporation of cargo into these membrane subdomains. We performed a floatation assay to verify whether the introduction of MAL/VIP17 into LLC-PK1 cells induces incorporation of c-NKCC2 into the DRMs. By convention, DRMs are considered to be membrane domains that are insoluble when lysed at 4°C in 1% Triton X-100. Indeed, we first performed the floatation assay in these experimental conditions. However, we found that in MAL/VIP17-negative LLC-PK1 cells only a small pool of the cotransporter is associated with Triton-resistant DRMs and that the coexpression of MAL/VIP17 with c-NKCC2 in these cells did not result in a further recruitment of c-NKCC2 into DRMs (Supplemental Figure 3A).

Because MAL/VIP17 and c-NKCC2 coimmunoprecipitated when cells were lysed in a mild detergent such as CHAPS, we performed the floatation assay after extracting the cells in cold 2% CHAPS (see *Materials and Methods*). As shown in Figure 6A, MAL/VIP17 and flotillin-2 behaved similarly thus floating exclusively to the lighter fractions, demonstrating that they were included in the DRMs (Figure 6A, Flo-2, MAL/VIP17). Moreover, c-NKCC2 is mainly expressed in the lighter fractions regardless of whether the MAL/VIP17 is ectopically expressed, suggesting that c-NKCC2 per se is included in CHAPS-resistant DRMs in LLC-PK1 cells (Figure 6A, c-NKCC2). We obtained the same results in lysates from rat kidney medullae (Supplemental Figure 3B).

We next investigated whether p-NKCC2, as well as the total NKCC2, is preferentially associated with DRMs and whether the presence of MAL/VIP17 might regulates this association. Because the detection of phosphorylated NKCC2 with R5 antibody requires a rapid processing of the sample, we addressed this issue by a detergent solubility assay (see *Materials and Methods*).

As shown in Figure 6B, p-NKCC2 was mainly expressed in the insoluble fraction regardless of whether MAL/VIP17 is ectopically expressed (Figure 6B, p-NKCC2). The same samples were assayed for the presence of flotillin-2 and MAL/VIP17. Both Flo-2 and MAL/VIP17 were expressed only in the insoluble fraction, indicating that this experimental procedure can actually separate rafts versus nonrafts membranes (Figure 6B, Flo-2, MAL/VIP17).

The samples were then probed with T4 to visualize the distribution of the total NKCC2 among the insoluble- and soluble-detergent fractions. As shown in Figure 6B, the total c-NKCC2 behaved similarly to p-NKCC2, confirming the results obtained in the floatation assay (Figure 6B, c-NKCC2).

Overall, the experiments conducted in LLC-PK1 and MDCK cells indicate that 1) a 150-amino acid stretch of NKCC2 C-terminal tail is involved in the interaction with MAL/VIP17, 2) MAL/VIP17 is not involved in the apical surface delivery of c-NKCC2 but rather in the stabilization of the cotransporter at the apical membrane domain, 3) this coincides with an increase in the phosphorylation level of c-NKCC2 in both basal and activating conditions, and 4) MAL/VIP17 does not induce any further recruitment of c-NKCC2 into a subpopulation of DRMs.

### *NKCC2 Expression in MAL/VIP17-overexpressing Transgenic Mice*

Transgenic animals are widely used to understand the physiological role and regulation of several membrane proteins. Because MAL/VIP17 has been characterized as an additional myelin component (Frank *et al*., 1999; Erne *et al*., 2002), transgenic mice overexpressing MAL/VIP17 have been generated to gain more insight into the functional roles of MAL/VIP17 in myelin formation (Frank *et al*., 2000). Beside the myelin alteration in the CNS, Frank *et al*. (2000) found the formation of large cysts in the kidney tubules of these transgenic mice. This observation is consistent with dramatic amplification of the apical surface of the renal epithelial cells and with the hypothesis that MAL/VIP17 plays an important role in apical sorting or in maintaining the stability of the apical membranes.

We analyzed the expression and regulation of NKCC2 in the kidneys of these mice. Western blot analysis of whole kidney lysates clearly showed an increase in the extent of NKCC2 glycosylation as well as MAL/VIP17 expression in transgenic mice compared with wild-type littermates (Figure 7A, gly-NKCC2, MAL/VIP17). Densitometric analysis of the broad band centered at ~160 kDa, normalized to the

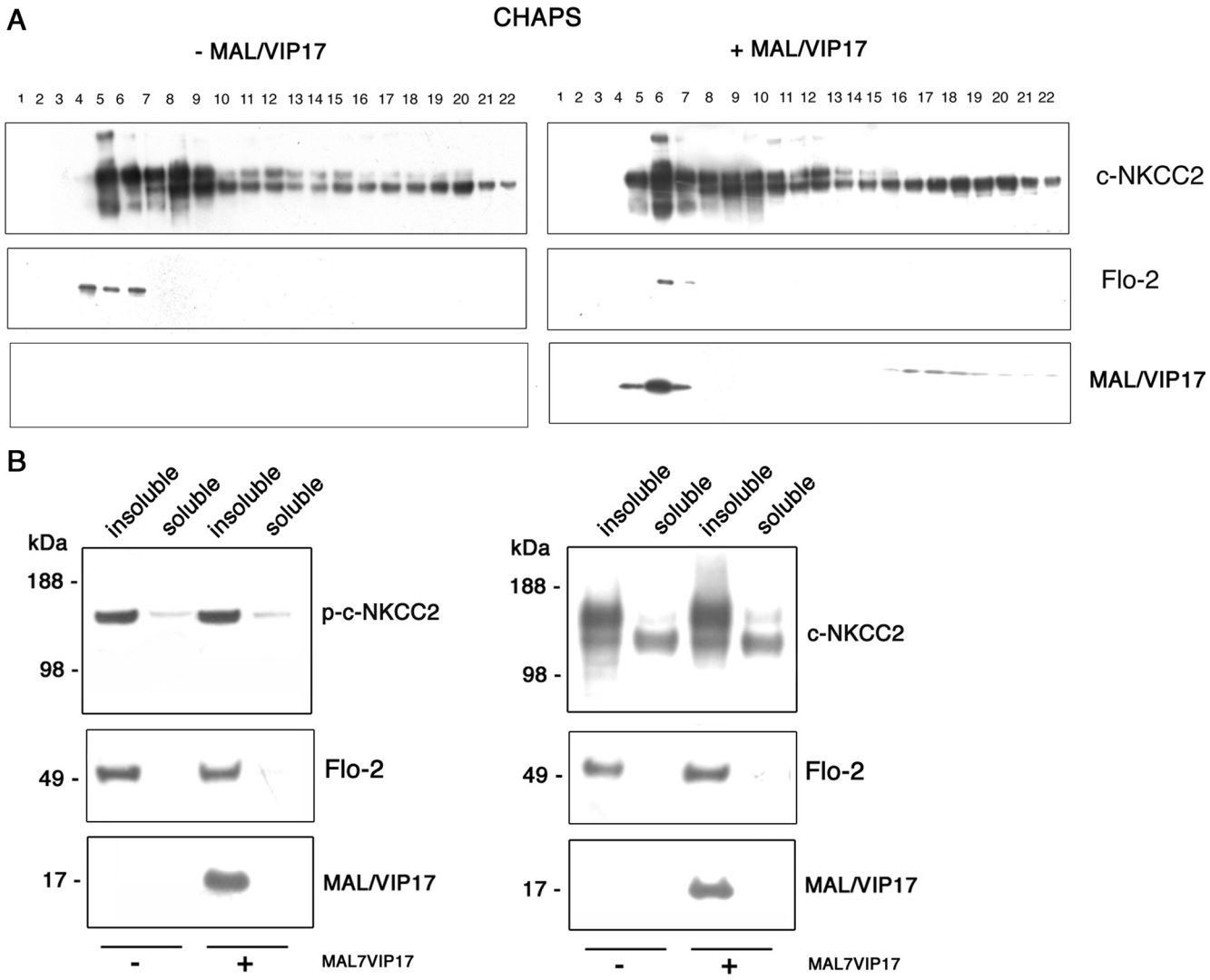


**Figure 6.** Floatation and detergent solubility assays in LLC-PK1 cells transfected with c-NKCC2 alone or in combination with MAL/VIP17. (A) LLC-PK1 cells were lysed in 2% CHAPS at 4°C. Lysates were then subjected to floatation assay as described in *Materials and Methods*. Twenty-two fractions, taken from the top to the bottom of the gradient, were subjected to immunoblotting with antibodies specific for the membrane proteins indicated on the right. These data are representative of three independent experiments. The expression of MAL/VIP17 did not induce any further recruitment of c-NKCC2 into DRMs. (B) LLC-PK1 cells were lysed in 2% CHAPS at 4°C. Lysates were then fractionated into supernatant (soluble fraction) and pellet (insoluble fraction), and equal amounts of total proteins was analyzed by SDS-PAGE followed by immunoblotting with antibodies specific for the membrane proteins indicated on the right. The expression of MAL/VIP17 did not induce any further recruitment of p-c-NKCC2 into DRMs.

corresponding actin band, showed that the band corresponding to glycosylated NKCC2 increased by ~40% in transgenic mice compared with control mice (Figure 7A′). To verify that the broad band centered at 160 kDa actually corresponds to the glycosylated form of NKCC2, we treated kidney lysates from MAL/VIP17 transgenic mice with peptide-$N^{-}$-(*N*-acetyl-$\beta$-glucosaminyl)asparagine amidase (PNGase F). As shown in Figure 7A″, glycosidase treatment shifted the molecular mass of the NKCC2-immunoreactive broad band to ~135 kDa. Moreover, Western blotting analysis of whole kidney lysates using the R5 antibody showed that NKCC2 was more heavily phosphorylated in transgenic mice compared with control mice (Figure 7B). Densitometric analysis of the R5-reactive band clearly showed in increase in NKCC2 phosphorylation by ~40% in transgenic mice (Figure 7B′).

Accordingly, immunofluorescence experiments using R5 antibody showed a strong labeling of the cells lining the cysts, as well as the apical membrane of TAL tubules, in transgenic mice. In contrast, very faint or absent labeling was found in control mice (Figure 7C). The increase in both NKCC2 glycosylation and phosphorylation observed in MAL/VIP17-overexpressing mice might be consistent with an increase in NKCC2 membrane stability in those animals, corroborating the results obtained in MAL/VIP17-expressing LLC-PK1 cells.

## DISCUSSION

We find that in the kidney, the NKCC2 cotransporter colocalizes and interacts with MAL/VIP17, which shares features with members of the tetraspan and MARVEL family of

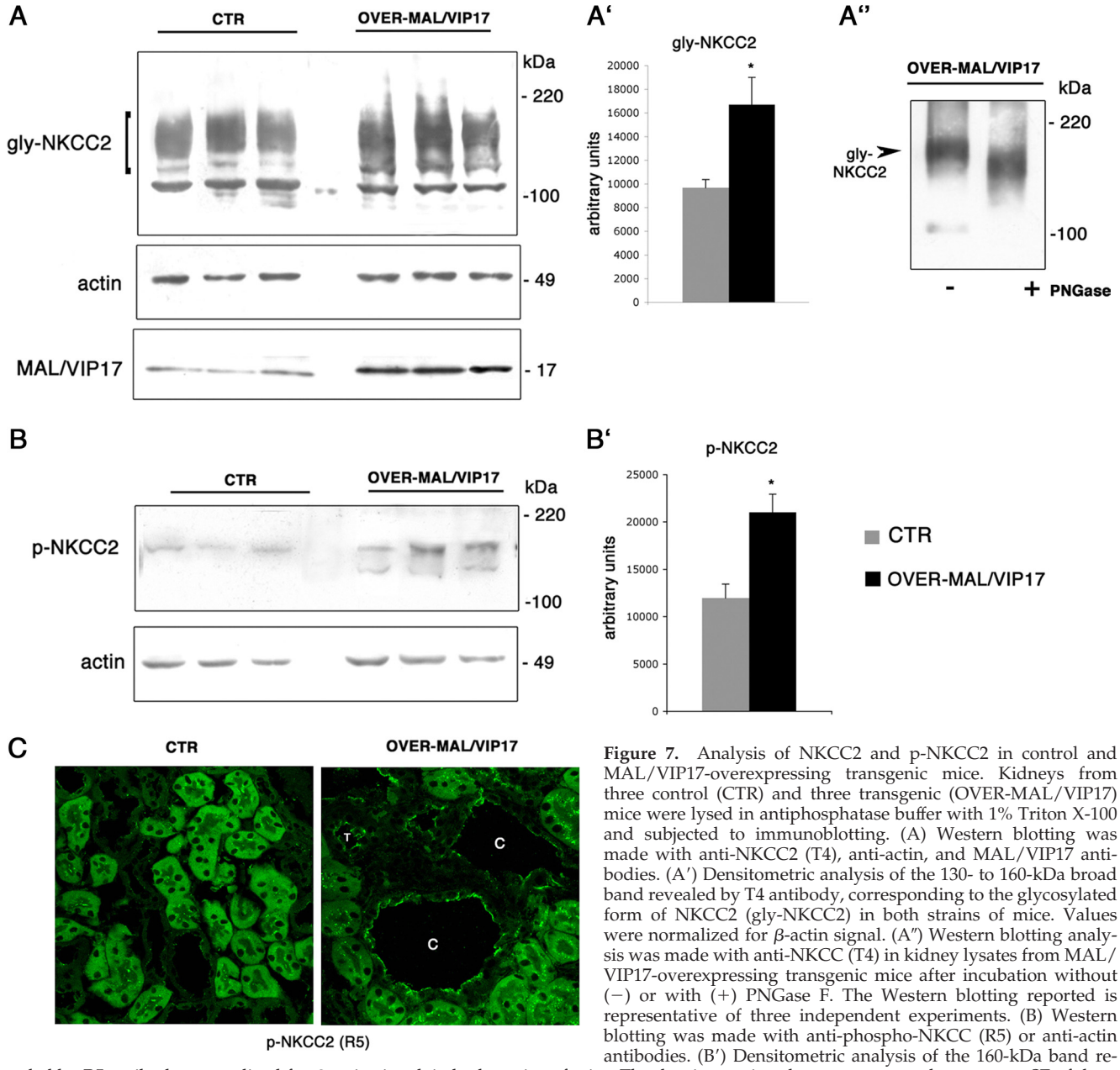


**Figure 7.** Analysis of NKCC2 and p-NKCC2 in control and MAL/VIP17-overexpressing transgenic mice. Kidneys from three control (CTR) and three transgenic (OVER-MAL/VIP17) mice were lysed in antiphosphatase buffer with 1% Triton X-100 and subjected to immunoblotting. (A) Western blotting was made with anti-NKCC2 (T4), anti-actin, and MAL/VIP17 antibodies. (A′) Densitometric analysis of the 130- to 160-kDa broad band revealed by T4 antibody, corresponding to the glycosylated form of NKCC2 (gly-NKCC2) in both strains of mice. Values were normalized for $\beta$-actin signal. (A″) Western blotting analysis was made with anti-NKCC (T4) in kidney lysates from MAL/VIP17-overexpressing transgenic mice after incubation without (−) or with (+) PNGase F. The Western blotting reported is representative of three independent experiments. (B) Western blotting was made with anti-phospho-NKCC (R5) or anti-actin antibodies. (B′) Densitometric analysis of the 160-kDa band revealed by R5 antibody, normalized for $\beta$-actin signal, in both strains of mice. The densitometric values are expressed as mean ± SE of three independent experiments. Student's *t* test, *$p < 0.001$. (C) Sections from paraformaldehyde-fixed kidneys of control or transgenic mice were subjected to immunofluorescence with R5 antibody. Images were collected with a confocal laser-scanning microscope from kidneys of three control and three transgenic mice. Two representative pictures are presented. The staining with R5 was present in cells lining the cysts (C) as well as in normal tubules (T) in MAL/VIP17-transgenic mice (OVER-MAL/VIP17). The staining is absent in kidneys from control mice.

proteins. This observation suggests that these families of polypeptides constitute a new collection of membrane proteins involved in regulating the distribution and function of renal transporters.

Several of the tetraspan proteins were first identified as surface antigens on cells of the immune system, as reflected in their inclusion in the "cluster of differentiation (CD)" system of nomenclature (Hammond *et al.*, 1998; Levy *et al.*, 1998). The expression of the tetraspan proteins has been found not to be limited, however, to cells of bone marrow origin. Most of the tetraspans are found in a wide variety of cell types, including epithelia, neurons, glia, endothelia, and smooth and striated muscle (Okochi *et al.*, 1999; Fradkin *et al.*, 2002; Zhang *et al.*, 2009) where they are involved in several physiological events such as cell motility and adhesion, fertility, vision, and brain development (Caplan *et al.*, 2007; Charrin *et al.*, 2009).

Here, we identified a functional role for the interaction between NKCC2 and MAL/VIP17 in regulating the surface expression of NKCC2. This finding is novel and interesting, because very little is known about NKCC2 intracellular trafficking, membrane stability and regulation due to the difficulty inherent in stably expressing NKCC2 in epithelial cells.

The N-terminal tail of NKCC2 is a critical region of the protein that is required for its stable expression in epithelial cells (Isenring *et al.*, 1998). Thus, we previously generated a

chimeric NKCC construct in which the apical sorting determinants of NKCC2, identified in its C terminus, has been exchanged into the NKCC1 backbone (Carmosino *et al*., 2008). The resulting chimera (that we refer to as c-NKCC2 here) is selectively expressed at the apical domain in epithelial cells and it is functionally active, thus rendering it a useful tool for studying the regulation of NKCC2 in an epithelial cell system.

Experiments performed in LLC-PK1 cells cotransfected with c-NKCC2 and MAL/VIP17 demonstrated that the chimera selectively colocalizes at the apical membrane and interacts with MAL/VIP17.

Interactions of tetraspan family proteins with partner proteins can be formed via different structural domains. For example, CD81 associates with the extracellular domain of immunoglobulin CD19 (Matsumoto *et al*., 1993) and with the intracellular domain of another partner immunoglobulin EWI-2 (Stipp *et al*., 2001). Moreover, CD151 interacts with the extracellular domains of $\alpha$3-integrin (Yauch *et al*., 2000).

Taking advantage of the chimeric NKCC2 protein used in this work, we have been able to map in the NKCC2 the region of its interaction with MAL/VIP17. NKCC1 was not able to coimmunoprecipitate with MAL/VIP17 even when the two proteins colocalize at the plasma membrane in HEK cells, suggesting that the 150-C–terminal amino acid stretch of NKCC2 present in the chimeric construct is involved in the interaction with MAL/VIP17.

Localization experiments showed that c-NKCC2 is delivered to the apical membrane in LLC-PK1 cells independently of MAL/VIP17 ectopic expression, suggesting that MAL/VIP17 is not required for the apical sorting of NKCC2. It has been demonstrated previously that MAL/VIP17 plays an important role in the transport of apical proteins from the *trans*-Golgi network to the apical plasma membrane in MDCK cells. The expression of antisense RNA directed against MAL/VIP17 in MDCK cells caused accumulation in the Golgi and/or impaired apical transport of different apical protein markers, such as influenza virus hemagglutinin, the secretory protein clusterin (gp8O), the transmembrane protein gpll4, and a glycosylphosphatidylinositol-anchored protein (Cheong *et al*., 1999). However, we showed in this paper that knockdown of MAL/VIP17 expression by siRNA did not affect the apical sorting of NKCC2 in MDCK cells.

Moreover, it is also worth noting that both LLC-PK1 cells and the Caco-2 human colon carcinoma cell line (de Marco *et al*., 2002) express no endogenous MAL/VIP17, although the influenza HA protein is still sorted to the apical plasma membrane in these cell types (Roush *et al*., 1998; Riento *et al*., 2000). Rather, we demonstrated that the interaction with MAL/VIP17 stabilizes c-NKCC2 at the apical membrane of LLC-PK1 and MDCK cells by inhibiting the steady-state rate of endocytosis of this protein.

This result is in agreement with the previous observation that the interaction with MAL/VIP17 slows the internalization of AQP2, resulting in an increase in the population of this water channel that is present in the apical membrane in the absence of hormonal stimulation (Kamsteeg *et al*., 2007). Moreover, using the R5 antibody that is specifically directed against phosphorylated NKCCs, we showed that the stabilization of c-NKCC2 at the apical membrane of MAL/VIP17 expressing LLC-PK1 coincides with an increase in the extent of cotransporter phosphorylation.

It has been demonstrated that the activation of NKCC cotrasporters occurs upon their phosphorylation at three conserved threonines in the N terminus. The reactivity of a polyclonal antibody directed against these phospho-threonines (R5 antibody) with NKCCs directly mirrors their functional activation as assayed by rubidium fluxes (Flemmer *et al*., 2002). Thus, we can speculate that the increase in the extent of NKCC2 phosphorylation observed after the ectopic expression of MAL/VIP17 in LLC-PK1 cells (either in steady state or under activating conditions), coincides with an increase in NKCC2 activation. Possible explanations for the increased phosphorylation of c-NKCC2 in MAL/VIP17-expressing LLC-PK1 cells include 1) MAL/VIP17 preferentially interacts with phosphorylated c-NKCC2, or 2) MAL/VIP17 also binds to elements of the NKCC2 activation machinery.

We tested the first possibility by comparing the amounts of c-NKCC2 present in the MAL/VIP17 immunoprecipitates in the control condition and after low $Cl^-$ preincubation. The phosphorylation of the cotransporter after incubation in low Cl solution did not change its affinity for MAL/VIP17. Intracellular chloride depletion activates NKCC2 by promoting the phosphorylation of three highly conserved threonines (96, 101, and 111) in the amino terminus. The chloride-sensitive activation of NKCC2 requires its interaction with two serine-threonine kinases, WNK3 (with-no-lysine kinase) and SPAK (a Ste20-type kinase). WNK3 is positioned upstream of SPAK and seems to be the chloride-sensitive kinase (Ponce-Coria *et al*., 2008). Moreover, a binding site for the protein-phoshatase-1 has been identified in the N terminus of NKCC1, suggesting a crucial role for it in the regulation of NKCC1. Interestingly, we found that neither the SPAK kinase nor the protein phosphatase-1, the major players in the NKCC activation, coimmunoprecipitate with MAL/VIP17 (Supplemental Figure 2). Thus, we conclude that the observed increase in the fraction of phosphorylated NKCC2 may be attributable to the stabilization of the cotransporter at cell surface.

More interestingly, we showed that both glycosylation and phosphorylation patterns of NKCC2 were significantly increased in MAL/VIP17-overexpressing transgenic mice compared with the their controls. MAL/VIP17-overexpresing mice develop dramatically amplified renal epithelial cell apical membranes as well as cysts in the tubular system of the kidney, consistent with an important role of MAL/VIP17 in the genesis and development of apical plasma membranes in the kidney (Frank *et al*., 2000).

It has been demonstrated that the glycosylation of NKCC2 is necessary for the correct surface expression of the cotransporter and for the stabilization of its functional conformation (Paredes *et al*., 2006). Indeed, the increase in the extent of NKCC2 glycosylation and phosphorylation observed in MAL/VIP17-overexpressing mice might be consistent with an increase in the NKCC2 membrane stability. Further studies are needed to identify the molecular mechanism by which MAL/VIP17 inhibits NKCC2 internalization.

One possibility is that NKCC2 phosphorylation may play a role in the NKCC2 internalization. In fact, Western blotting with the R5 antibody did not detect phosphorylated NKCC2 in the endocytosed material in the presence or absence of MAL/VIP17 expression (data not shown). This may indicate that only nonphosphorylated NKCC2 is subject to endocytosis and that the phosphorylated form is not a substrate for internalization. If this is the case, the surface stabilization of NKCC2 induced by MAL/VIP17 expression may be due directly to the effects of MAL/VIP17 expression on NKCC2 phosphorylation. It is also possible, however, that the quantity of p-NKCC2 present in the endocytosed pool is below our limit of detection with the R5 antibody. Future experiments are required to choose among these possibilities.

Because MAL/VIP17 associates with sphingolipid-cholesterol rafts, another possibility is that MAL/VIP17 recruits its

interacting partners into these membrane domains. We showed here that NKCC2 is mainly expressed in mild detergent-resistant membrane domains in both LLC-PK1 cells and rat kidney medullae.

Interestingly, the expression of MAL/VIP17 in LLC-PK1 cells did not induce any further appreciable recruitment of c-NKCC2 into DRMs. Thus, the presence of NKCC2 in these membrane subdomains seems to be independent of MAL/VIP17.

It is believed that MAL/VIP17 plays its role in apical sorting processes by recruiting apical cargo into DRMs (Cheong *et al*., 1999; Puertollano *et al*., 1999). However, approximately half of the proteins that have been shown to require MAL/VIP17 for their apical sorting are not found in these DRMs (Martin-Belmonte *et al*., 2000, 2001). Therefore, we and others (Kamsteeg *et al*., 2007) suggest that one role of MAL/VIP17 in the apical sorting may be attributable to the stabilization and retention of MAL/VIP17 partner proteins at the apical surface after their initial apical delivery.

The predicted membrane-spanning helices of MAL/VIP17 constitute the MARVEL domain, which is found in ~20 open reading frames in the human genome (Sánchez-Pulido *et al*., 2002). The MARVEL domain is also found in the tight junction-localized protein occludin and in the synaptic-membrane-localized proteins synaptophysin and synaptogyrin. Thus, a common feature of proteins containing the MARVEL domain is localization to specialized domains within surface membranes.

Moreover, there is evidence for a potential role for MAL in the formation and stabilization of membrane domains that may potentially serve as apical sorting platforms, and as a possible membrane-thickness–stabilizing entity (Goldstein Magal *et al*., 2009). Indeed, we cannot exclude that MAL/VIP17 recruits the NKCC2 cotransporter into a MAL/VIP17-enriched specialized membrane domain in which additional partner proteins are included and involved in NKCC2 regulation. Proteomic approaches are in progress to identify other components of the MAL/VIP17 "interactome" in the kidney.

In conclusion, we identified the tetraspan-member family MAL/VIP17 as new player in the regulation of the functional expression of NKCC2 at the apical plasma membrane in the kidney. The interaction between MAL/VIP17 and NKCC2 might play an important role in the physiological regulation of body salt and water homeostasis as well as in the pathogenesis of hypertension.

## ACKNOWLEDGMENTS

We thank Vanathy Rajendran (Department of Cellular and Molecular Physiology, Yale University School of Medicine) for experimental assistance. This research was supported by the Italian grant PRIN 20078ZZMZW (to M. S.) and by Fondo per gli Investimenti della Ricerca di Base-Rete Nazionale di Proteomica (RBRN07BMCT_009).

## REFERENCES

Alvarez-Guerra, M., and Garay, R. P. (2002). Renal Na-K-Cl cotransporter NKCC2 in Dahl salt-sensitive rats. J. Hypertension *20*, 721–727.

Caplan, M. J., Kamsteeg, E. J., and Duffield, A. (2007). Tetraspan proteins: regulators of renal structure and function. Curr. Opin. Nephrol. Hypertens. *16*, 353–358.

Carmosino, M., Gimenez, I., Caplan, M., and Forbush, B. (2008). Exon loss accounts for differential sorting of Na-K-Cl cotransporters in polarized epithelial cells. Mol. Biol. Cell *19*, 4341–4351.

Charrin, S., le Naour, F., Silvie, O., Milhiet, P. E., Boucheix, C., and Rubinstein, E. (2009). Lateral organization of membrane proteins: tetraspanins spin their web. Biochem. J. *420*, 133–154.

Cheong, K. H., Zacchetti, D., Schneeberger, E. E., and Simons, K. (1999). MAL/VIP17/MAL, a lipid raft-associated protein, is involved in apical transport in MDCK cells. Proc. Natl. Acad. Sci. USA *96*, 6241–6248.

Darman, R. B., and Forbush, B. (2002). A regulatory locus of phosphorylation in the N terminus of the Na-K-Cl cotransporter, NKCC1. J. Biol. Chem. *277*, 37542–37550.

de Marco, M. C., Martin-Belmonte, F., Kremer, L., Albar, J. P., Correas, I., Vaerman, J. P., Marazuela, M., Byrne, J. A., and Alonso, M. A. (2002). MAL2, a novel raft protein of the MAL family, is an essential component of the machinery for transcytosis in hepatoma HepG2 cells. J. Cell Biol. *159*, 37–44.

Duffield, A., Kamsteeg, E. J., Brown, A. N., Pagel, P., and Caplan, M. J. (2003). The tetraspanin CD63 enhances the internalization of the H,K-ATPase beta-subunit. Proc. Natl. Acad. Sci. USA *100*, 15560–15565.

Erne, B., Sansano, S., Frank, M., and Schaeren-Wiemers, N. (2002). Rafts in adult peripheral nerve myelin contain major structural myelin proteins and myelin and lymphocyte protein (MAL) and CD59 as specific markers. J. Neurochem. *82*, 550–562.

Flemmer, A. W., Gimenez, I., Dowd, B. F., Darman, R. B., and Forbush, B. (2002). Activation of the Na-K-Cl cotransporter NKCC1 detected with a phospho-specific antibody. J. Biol. Chem. *277*, 37551–37558.

Fradkin, L. G., Kamphorst, J. T., DiAntonio, A., Goodman, C. S., and Noordermeer, J. N. (2002). Genomewide analysis of the *Drosophila* tetraspanins reveals a subset with similar function in the formation of the embryonic synapse. Proc. Natl. Acad. Sci. USA *99*, 13663–13668.

Frank, M., Atanasoski, S., Sancho, S., Magyar, J. P., Rulicke, T., Schwab, M. E., and Suter, U. (2000). Progressive segregation of unmyelinated axons in peripheral nerves, myelin alterations in the CNS, and cyst formation in the kidneys of myelin and lymphocyte protein-overexpressing mice. J. Neurochem. *75*, 1927–1939.

Frank, M., Schaeren-Wiemers, N., Schneider, R., and Schwab, M. E. (1999). Developmental expression pattern of the myelin proteolipid MAL indicates different functions of MAL for immature Schwann cells and in a late step of CNS myelinogenesis. J. Neurochem. *73*, 587–597.

Frank, M., van der Haar, M. E., Schaeren-Wiemers, N., and Schwab, M. E. (1998). rMAL is a glycosphingolipid-associated protein of myelin and apical membranes of epithelial cells in kidney and stomach. J. Neurosci. *18*, 4901–4913.

Gimenez, I., and Forbush, B. (2003). Short-term stimulation of the renal Na-K-Cl cotransporter (NKCC2) by vasopressin involves phosphorylation and membrane translocation of the protein. J. Biol. Chem. *278*, 26946–26951.

Goldstein Magal, L., Yaffe, Y., Shepshelovich, J., Aranda, J. F., de Marco, M. D., Gaus, K., Alonso, M. A., and Hirschberg, K. (2009). Clustering and lateral concentration of raft lipids by the MAL protein. Mol. Biol. Cell *20*, 3751–3762.

Hammond, C., Denzin, L. K., Pan, M., Griffith, J. M., Geuze, H. J., and Cresswell, P. (1998). The tetraspan protein CD82 is a resident of MHC class II compartments where it associates with HLA-DR, -DM, and -DO molecules. J. Immunol. *161*, 3282–3291.

Isenring, P., Jacoby, S. C., Payne, J. A., and Forbush, B., 3rd. (1998). Comparison of Na-K-Cl cotransporters. NKCC1, NKCC2, and the HEK cell Na-L-Cl cotransporter. J. Biol. Chem. *273*, 11295–11301.

Kamsteeg, E. J., Duffield, A. S., Konings, I. B., Spencer, J., Pagel, P., Deen, P. M., and Caplan, M. J. (2007). MAL decreases the internalization of the aquaporin-2 water channel. Proc. Natl. Acad. Sci. USA *104*, 16696–16701.

Levy, S., Todd, S. C., and Maecker, H. T. (1998). CD81 (TAPA-1): a molecule involved in signal transduction and cell adhesion in the immune system. Annu. Rev. Immunol. *16*, 89–109.

Liedtke, C. M., Wang, X., and Smallwood, N. D. (2005). Role for protein phosphatase 2A in the regulation of Calu-3 epithelial Na+-K+-2Cl-, type 1 co-transport function. J. Biol. Chem. *280*, 25491–25498.

Lin, D., Kamsteeg, E. J., Zhang, Y., Jin, Y., Sterling, H., Yue, P., Roos, M., Duffield, A., Spencer, J., Caplan, M., and Wang, W. H. (2008). Expression of tetraspan protein CD63 activates protein-tyrosine kinase (PTK) and enhances the PTK-induced inhibition of ROMK channels. J. Biol. Chem. *283*, 7674–7681.

Martin-Belmonte, F., Arvan, P., and Alonso, M. A. (2001). MAL mediates apical transport of secretory proteins in polarized epithelial Madin-Darby canine kidney cells. J. Biol. Chem. *276*, 49337–49342.

Martin-Belmonte, F., Puertollano, R., Millan, J., and Alonso, M. A. (2000). The MAL proteolipid is necessary for the overall apical delivery of membrane proteins in the polarized epithelial Madin-Darby canine kidney and Fischer rat thyroid cell lines. Mol. Biol. Cell *11*, 2033–2045.

Matsumoto, A. K., Martin, D. R., Carter, R. H., Klickstein, L. B., Ahearn, J. M., and Fearon, D. T. (1993). Functional dissection of the CD21/CD19/TAPA-1/Leu-13 complex of B lymphocytes. J. Exp. Med. *178*, 1407–1417.

Okochi, H., Mine, T., Nashiro, K., Suzuki, J., Fujita, T., and Furue, M. (1999). Expression of tetraspans transmembrane family in the epithelium of the gastrointestinal tract. J. Clin. Gastroenterol. *29*, 63–67.

Pagel, P., Zatti, A., Kimura, T., Duffield, A., Chauvet, V., Rajendran, V., and Caplan, M. J. (2003). Ion pump-interacting proteins: promising new partners. Ann. NY Acad. Sci. *986*, 360–368.

Paredes, A., Plata, C., Rivera, M., Moreno, E., Vazquez, N., Munoz-Clares, R., Hebert, S. C., and Gamba, G. (2006). Activity of the renal Na+-K+-2Cl-cotransporter is reduced by mutagenesis of N-glycosylation sites: role for protein surface charge in Cl- transport. Am. J. Physiol. Renal Physiol. *290*, F1094–F1102.

Ponce-Coria, J., *et al*. (2008). Regulation of NKCC2 by a chloride-sensing mechanism involving the WNK3 and SPAK kinases. Proc. Natl. Acad. Sci. USA *105*, 8458–8463.

Pressler, C. A., Heinzinger, J., Jeck, N., Waldegger, P., Pechmann, U., Reinalter, S., Konrad, M., Beetz, R., Seyberth, H. W., and Waldegger, S. (2006). Late-onset manifestation of antenatal Bartter syndrome as a result of residual function of the mutated renal Na+-K+-2Cl- co-transporter. J. Am. Soc. Nephrol. *17*, 2136–2142.

Procino, G., Barbieri, C., Carmosino, M., Rizzo, F., Valenti, G., and Svelto, M. (2010). Lovastatin-induced cholesterol depletion affects both apical sorting and endocytosis of aquaporin-2 in renal cells. Am. J. Physiol. Renal. Physiol. *298*, F266–F278.

Puertollano, R., Martin-Belmonte, F., Millan, J., de Marco, M. C., Albar, J. P., Kremer, L., and Alonso, M. A. (1999). The MAL proteolipid is necessary for normal apical transport and accurate sorting of the influenza virus hemagglutinin in Madin-Darby canine kidney cells. J. Cell Biol. *145*, 141–151.

Ramnarayanan, S. P., Cheng, C. A., Bastaki, M., and Tuma, P. L. (2007). Exogenous MAL reroutes selected hepatic apical proteins into the direct pathway in WIF-B cells. Mol. Biol. Cell *18*, 2707–2715.

Riento, K., Kauppi, M., Keranen, S., and Olkkonen, V. M. (2000). Munc18–2, a functional partner of syntaxin 3, controls apical membrane trafficking in epithelial cells. J. Biol. Chem. *275*, 13476–13483.

Roush, D. L., Gottardi, C. J., Naim, H. Y., Roth, M. G., and Caplan, M. J. (1998). Tyrosine-based membrane protein sorting signals are differentially interpreted by polarized Madin-Darby canine kidney and LLC-PK1 epithelial cells. J. Biol. Chem. *273*, 26862–26869.

Sánchez-Pulido, L., Martín-Belmonte, F., Valencia, A., and Alonso, M. A. (2002). MARVEL: a conserved domain involved in membrane apposition events. Trends Biochem. Sci. *27(12)*, 599–601.

Simon, D. B., Karet, F. E., Hamdan, J. M., DiPietro, A., Sanjad, S. A., and Lifton, R. P. (1996). Bartter's syndrome, hypokalaemic alkalosis with hypercalciuria, is caused by mutations in the Na-K-2Cl cotransporter NKCC2. Nat. Genet. *13*, 183–188.

Sonalker, P. A., Tofovic, S. P., and Jackson, E. K. (2004). Increased expression of the sodium transporter BSC-1 in spontaneously hypertensive rats. J. Pharmacol. Exp. Ther. *311*, 1052–1061.

Sonalker, P. A., Tofovic, S. P., and Jackson, E. K. (2007). Cellular distribution of the renal bumetanide-sensitive Na-K-2Cl cotransporter BSC-1 in the inner stripe of the outer medulla during the development of hypertension in the spontaneously hypertensive rat. Clin. Exp. Pharmacol. Physiol. *34*, 1307–1312.

Stipp, C. S., Kolesnikova, T. V., and Hemler, M. E. (2001). EWI-2 is a major CD9 and CD81 partner and member of a novel Ig protein subfamily. J. Biol. Chem. *276*, 40545–40554.

Yauch, R. L., Kazarov, A. R., Desai, B., Lee, R. T., and Hemler, M. E. (2000). Direct extracellular contact between integrin alpha(3)beta(1) and TM4SF protein CD151. J. Biol. Chem. *275*, 9230–9238.

Zhang, F., Kotha, J., Jennings, L. K., and Zhang, X. A. (2009). Tetraspanins and vascular functions. Cardiovasc. Res. *83*, 7–15.